Methane dehydro-aromatization over a Mo/phosphoric rare earth-containing penta-sil type zeolite in the absence of oxygen

Yuying Shu, Ding Ma, Xinhe Bao and Yide Xu *

State Key Laboratory of Catalysis, Dalian Institute of Chemical Physics, Chinese Academy of Sciences, 457 Zhongshan Road, PO Box 110, Dalian 116023, PR China
E-mail: xuyd@ms.dicp.ac.cn

Received 18 January 2000; accepted 11 April 2000

The dehydro-aromatization of methane over a Mo-modified penta-sil type high-silica zeolite containing phosphoric and rare earth oxide (abbreviated as Mo/HZRP-1) was investigated. As a modification of HZSM-5, HZRP-1 is also a good support for the preparation of Mo-based zeolite catalysts, and is active for methane dehydro-aromatization. Mo/HZRP-1 catalysts are more active at high Mo loadings compared with Mo/HZSM-5 catalysts. ^{27}Al MAS NMR spectra of Mo/HZRP-1 reveal that there are two kinds of framework Al in HZRP-1. It is suggested that only the tetrahedral coordinated Al atoms in the form of Al–O–Si species in the zeolite, in the proton forms, are responsible for the formation of aromatics.

Keywords: methane dehydro-aromatization, Mo/HZRP-1 catalyst, NH_3-TPD, ^{27}Al MAS NMR

1. Introduction

Recently, increasing attention has been paid to methane dehydro-aromatization in the absence of oxygen over Mo/HZSM-5 catalysts in the continuous flow mode [1]. This new approach may offer an alternative route not only for the study of methane activation, but also for the utilization of natural gas as the raw material for the production of aromatics and hydrogen. Although a great deal of work has been done on methane dehydro-aromatization, many problems remain to be solved both in academic research and possible industrial application.

In previous studies on this reaction, Solymosi et al. [2,3] and Lunsford et al. [4] suggested that Mo_2C on the external surface, formed during the initial stage of the reaction, is responsible for methane activation, and leads to the formation of C_2H_4. Recently, Lunsford et al. [5] further suggested that a coke-modified Mo_2C surface might be the active center for the reaction since they found that pre-formation of Mo_2C on the catalyst, without a coke deposit, did not completely eliminate the induction period. They believed that the clean surface of Mo_2C might be too reactive to form higher hydrocarbons. Later, Iglesia et al. [6] pointed out that during initial contact with CH_4 at 950 K, Mo^{6+} cations are converted to the oxycarbide species, MoO_xC_y, which activates CH_4. In our recent EPR study of the Mo species on the Mo/HZSM-5 catalyst [7], it was revealed that there are two kinds of Mo species. The first kind of Mo species is polynuclear and located on the external surface. The second kind of the Mo species is associated with the Al atom and most of them are in the channels of the zeolite. The former Mo species is easily to be reduced by CH_4, while it is difficult to reduce the latter one. Both these Mo species play an essential role in methane dehydro-aromatization.

In order to improve the selectivity to aromatics of Mo-modified zeolites, a variety of zeolites were screened as the support, and a kind of phosphoric and rare earth oxide-containing penta-sil type high-silica zeolite, which is a modification of HZSM-5, seems interesting and worthy of study. This kind of penta-sil type high-silica zeolite is commercially denoted as ZRP-1 in China and was developed by the Research Institute of Petroleum Processing [8]. It has an anhydrous chemical composition with the formula of $x\mathrm{RE_2O_3}{\cdot}y\mathrm{Na_2O}{\cdot}\mathrm{Al_2O_3}{\cdot}z\mathrm{SiO_2}$ (based on the mole ratios of oxides), with the range of $x = 0.01$–0.30, $y = 0.4$–1.0 and $z = 20$–60. It was suggested that the role of the phosphorus compounds and rare earth oxide, when this was used as a component of FCC catalysts, is to block the acid sites on the external surface and to adjust its acidity. In addition, there was a slight decrease in the channel size and the dealumination of the zeolite with simultaneous formation of different P- and/or Al-containing compounds within the pore system. P- and/or rare earth oxide-containing zeolite may modify the acid sites of the zeolite and, therefore, suppresses coke formation. On the other hand, since almost all researchers have used HZSM-5 as the support till now, it is also beneficial to accumulate more experimental results from different Mo-modified zeolites. In this paper, the catalytic performance of methane dehydro-aromatization over the Mo/HZRP-1 catalysts is reported and compared with the Mo/HZSM-5 catalysts. Moreover, characterization of the Mo/HZRP-1 catalysts by ^{27}Al and ^{31}P MAS NMR measurements and the NH_3-TPD technique were conducted. A discussion with an attempt to correlate the catalytic perfor-

* To whom correspondence should be addressed.

mance of the Mo/HZRP-1 catalysts with their framework Al is also presented.

2. Experimental

2.1. Catalyst preparation

NaZRP-1 zeolite, supplied by the Research Institute of Petroleum Processing, has a SiO_2/Al_2O_3 ratio of 50. It consisted of $Na_2O < 0.1\%$, $Re_2O_3 \geqslant 0.8\%$, $P_2O_5 = 2.5$–5.0% and $Al_2O_3 = 5.0$–8.0%. The catalyst preparation followed the same procedure as reported in our previous paper [9]. The NaZRP-1 zeolite was first converted into its ammonium form by repeated ion exchanges with a 1 N NH_4NO_3 aqueous solution at about 368 K. It was then dried at 383 K overnight. Mo/HZRP-1 catalysts were prepared by impregnating NH_4ZRP-1 with a desirable amount of ammonium heptamolybdate (AHM) solution. They were dried and calcined at 773 K for 6 h. The samples were pressed, crushed and sorted into sizes of 20–60 mesh. Generally, the notation used for the catalyst is xMo/HZRP-1, where x denotes the Mo loading in weight percent.

2.2. Catalyst characterization

Specific surface area and average pore diameter of the samples were obtained by the BET method at liquid-nitrogen temperature of 78 K, taking a value of 0.162 nm^2 for the cross-sectional area of N_2. The measurement was performed with an ASAP-2000 equipment produced by Micromeritics and the data were processed and analyzed by an IBM computer.

XRD patterns were obtained on a D/max-rb X-ray diffractometer using Cu Kα radiation at room temperature and instrumental settings of 40 kV and 100 mA. The powder diffractograms of the samples were recorded over a range of 2θ values from 5° to 50°. The scanning rate was set at 5°/min. All XRD patterns were recorded, stored and processed by a computer system.

NH_3 temperature-programmed desorption (NH_3-TPD) was performed on a conventional set-up equipped with a thermal conductivity detector (TCD). The catalyst charge was 0.2 g with particle size of 20–60 mesh. The sample was first flushed with He (30 ml/min) at 873 K for 30 min, then cooled to 423 K and saturated with NH_3 until equilibrium. It was then flushed with He again until the integrator baseline was stable. NH_3-TPD was then promptly started at a heating rate of 15 K/min from 423 to 873 K. All NH_3-TPD profiles were deconvoluted into three peaks using a Gaussian and Lorentzian curve-fitting method.

^{27}Al and ^{31}P NMR measurements were performed on a Bruker DRX-400 spectrometer with MAS probe. The spin rate was 8 kHz for ^{27}Al and 4 kHz for ^{31}P MAS NMR measurements, respectively. The relaxation delay was 0.8 s for ^{27}Al and 2 s for ^{31}P. The sweep width was 23.8 kHz for ^{27}Al and for ^{31}P. 85% H_3PO_4 and $Al(H_2O)_6^{3+}$ were taken as an external reference of chemical shifts for ^{31}P and ^{27}Al, respectively.

2.3. Catalyst evaluation

Catalytic evaluation was performed in a 6.2 mm I.D. quartz tubular fixed-bed reactor, as described in [7]. Briefly, about 0.2 g catalyst was charged in the reactor and about 2 g of quartz chips was placed on the top of the catalyst bed to preheat the feed. A certain amount of N_2 (about 9.5 vol%) was mixed in the feed and used as an internal standard, as suggested by Lunsford et al. [4,5]. Gases used for preparing the N_2/CH_4 mixture and He used for pretreatment were all in UHP grade. All the gases were used without further purification. Typically, the catalytic test was carried out at atmospheric pressure and 973 K. The catalyst was first heated under He stream (15 ml/min) to 973 K and maintained at 973 K for 30 min. After the pretreatment, the N_2/CH_4 gas mixture was introduced into the reactor at a space velocity of 1500 ml/g_{cat} h. Hydrocarbons in the tail-gas were separated and analyzed by an on-line gas chromatograph (Shimadzu GC-9AM) equipped with a column of OV-101 on a 6201 support and a flame ionization detector (FID). A HayeSep-D column and a thermal conductivity detector (TCD) were equipped on the same gas chromatograph for the on-line separation and analysis of H_2, N_2, CO, CH_4, CO_2, C_2H_4, C_2H_6, etc. All reaction rates were expressed in nmol-CH_4/g_{cat} s. For simplicity, hereafter, r_{CH_4} denotes the depletion rate of CH_4, r_{CO}, r_{HC}, r_{BTX}, r_{NA} and r_C denote the CO, the C_2–C_4 hydrocarbon, the light aromatics (including benzene, toluene and xylene), the naphthalene and the carbonaceous deposits formation rate, respectively.

3. Results

3.1. Characterization of the Mo/HZRP-1 samples

Figure 1 shows the effect of Mo loading on the surface area and micropore volume of the Mo/HZRP-1 catalysts. The surface area decreases linearly with increasing Mo loading. Even at a Mo loading of as high as 20%, the

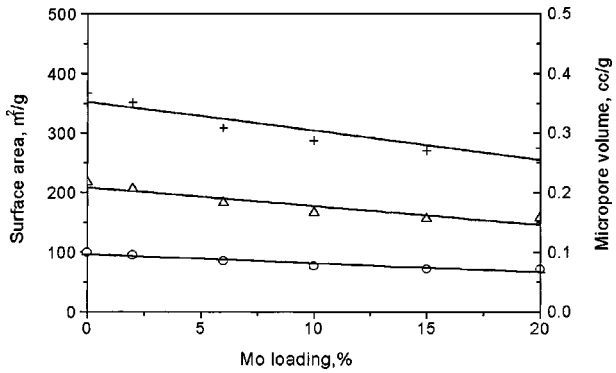

Figure 1. Effect of Mo loading on BET (+) and micro surface area (△), and micropore volume (○) of Mo/HZRP-1 catalysts.

corresponding surface area was about 275 m^2/g_{cat}, showing that the framework of HZRP-1 remains intact after the introduction of Mo species and that the Mo species are well dispersed on the surface. The micropore volume of HZRP-1 also decreases linearly after the introduction of Mo species. This indicates that part of the Mo species migrates into the channels of the HZRP-1 after calcination. Similar to the Mo/HZSM-5 catalysts reported in our previous study [9], Mo species are well-dispersed on/in the HZRP-1 and no MoO_3 phase could be clearly detected for the 10Mo/HZRP-1 catalyst. However, for a sample with the Mo loading higher than 10%, MoO_3 crystallites could be easily detected at 2θ value of 12.7°, 27.3° and 39.0° in the XRD patterns (see figure 2).

Figure 3 shows NH_3-TPD profiles of Mo/HZRP-1 catalysts with different Mo loadings. It also includes the curve-

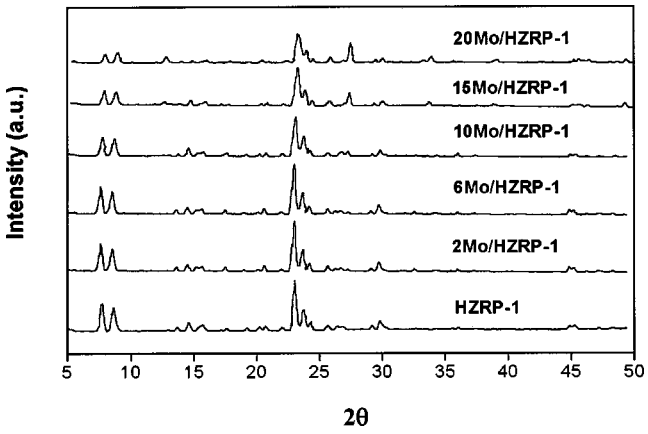

Figure 2. XRD profiles of HZRP-1 and Mo/HZRP-1 with different Mo loadings.

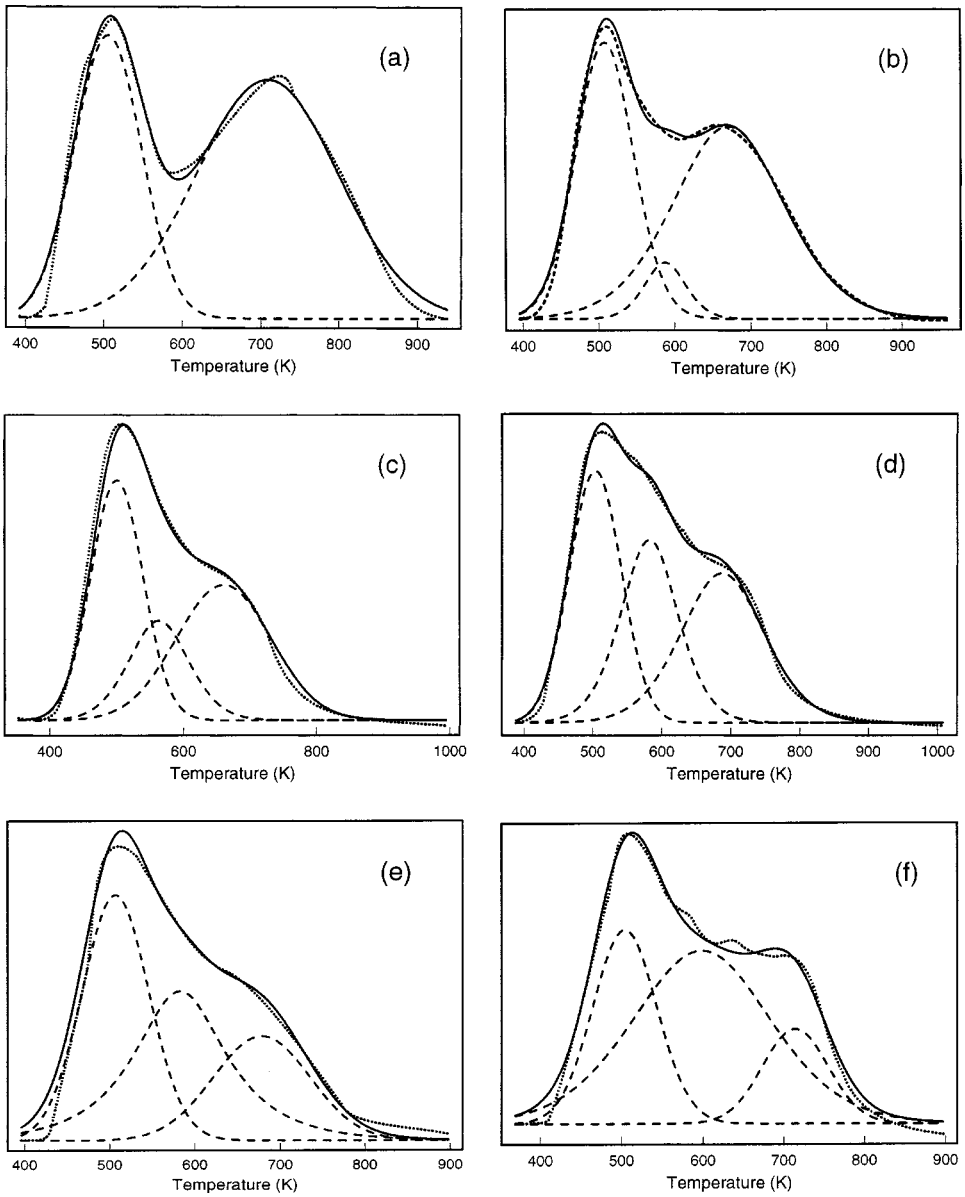

Figure 3. NH_3-TPD profiles recorded from Mo/HZRP-1 catalysts and the curve-fitting results: (a) HZRP-1, (b) 2Mo/HZRP-1, (c) 6Mo/HZRP-1, (d) 10Mo/HZRP-1, (e) 15Mo/HZRP-1 and (f) 20Mo/HZRP-1.

Table 1
Peak temperatures of NH_3-TPD spectra and the peak areas of Mo/HZRP-1 catalysts.

Sample	Peak L		Peak M		Peak H		Total
	Temp. (K)	Area	Temp. (K)	Area	Temp. (K)	Area	areas
HZRP-1	505	519	–	–	708	921	1440
2Mo	507	456	587	68	671	623	1147
6Mo	501	435	563	212	660	445	1092
10Mo	503	450	580	374	687	437	1261
15Mo	506	418	582	390	678	255	1063
20Mo	504	365	598	711	710	184	1260

fitting results. Two peaks can be observed on the NH_3-TPD profile recorded from the HZRP-1 zeolite. One is at 505 K (denoted as peak L), resulting from desorption of physisorbed NH_3 species or NH_3 species adsorbed on weak acid sites. The other is at 708 K (denoted as peak H), which is from desorption of NH_3 species adsorbed on strong acid sites. With an increase of Mo loading, both the areas of peak H and peak L decrease, but the areas corresponding to the peak L decrease more smoothly. Meanwhile, a new type of peak with medium strength, denoted as peak M, developed and the peak areas increase with Mo loading. Table 1 lists typical curve-fitting results of the Mo/HZRP-1 catalysts with different Mo loadings.

3.2. Methane dehydro-aromatization over Mo/HZRP-1 catalysts

Methane conversion, the formation rate of carbonaceous deposit, r_C, and other product formation rates, r_{CO}, r_{HC}, r_{BTX} and r_{NA}, after running the reaction for 30 min over Mo/HZRP-1 with different Mo loadings are given in figure 4. Methane conversion increases sharply with the introduction of Mo species if the Mo loading is less than 6%. Then, it increases slightly if the Mo loading is in the range from 6 to 20%. The rates r_{CO} and r_{HC} remain at relatively low levels and the rates r_{BTX} and r_{NA} remain at relatively high levels. r_{BTX} is the highest among all the product rates for the tested Mo/HZRP-1 catalysts. r_{BTX} increases remarkably with increasing Mo loading at first in the range of 0–6%, and then increases slightly up to a Mo loading of 20%.

Methane conversion and product formation rates over 6Mo/HZRP-1 and 20Mo/HZRP-1 catalysts as a function of running time are shown in figures 5 and 6, respectively. HZRP-1 shows no dehydro-aromatization activity at all, and the converted methane is solely transformed into carbonaceous deposit. On the 6Mo/HZRP-1 catalyst, the methane conversion, r_{BTX} and r_{NA} decrease, while they decrease more obviously over the 20Mo/HZRP-1 catalyst with increase of the running time. r_{BTX} decreases from 880 to 420 nmol/g_{cat} s on the 6Mo/HZRP-1 catalyst and from 920 to 340 nmol/g_{cat} s on the 20Mo/HZRP-1 catalyst after running the reaction for 6 h. At the same time, the r_{NA} decreases from 511 to 76 nmol/g_{cat} s on 6Mo/HZRP-1 and from 319 to 44 nmol/g_{cat} s on 20Mo/HZRP-1 catalyst. r_{CO} always decreases while r_{HC} always increases with the running time.

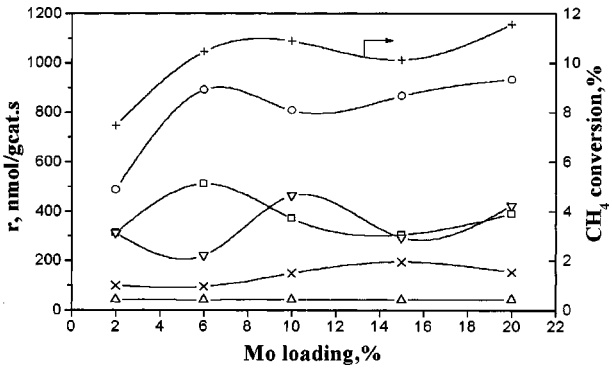

Figure 4. Effect of Mo loading on methane conversion (+) and product formation rates r_{CO} (×), r_{HC} (△), r_{BTX} (○), r_{NA} (□) and r_C (▽) over Mo/HZRP-1 catalysts after running 30 min.

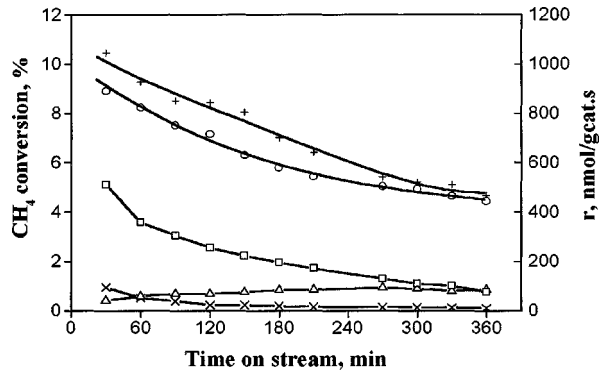

Figure 5. Catalytic performance of the 6Mo/HZRP-1 catalyst for methane dehydro-aromatization at 973 K as a function of time on stream: (+) conversion of methane, (×) r_{CO}, (△) r_{HC}, (○) r_{BTX} and (□) r_{NA}.

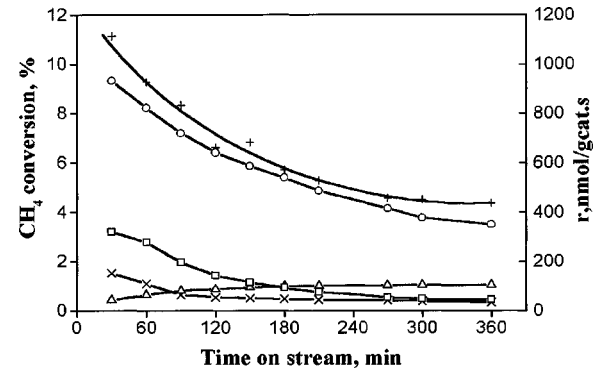

Figure 6. Catalytic performance of the 20Mo/HZRP-1 catalyst for methane dehydro-aromatization at 973 K as a function of time on stream: (+) conversion of methane, (×) r_{CO}, (△) r_{HC}, (○) r_{BTX} and (□) r_{NA}.

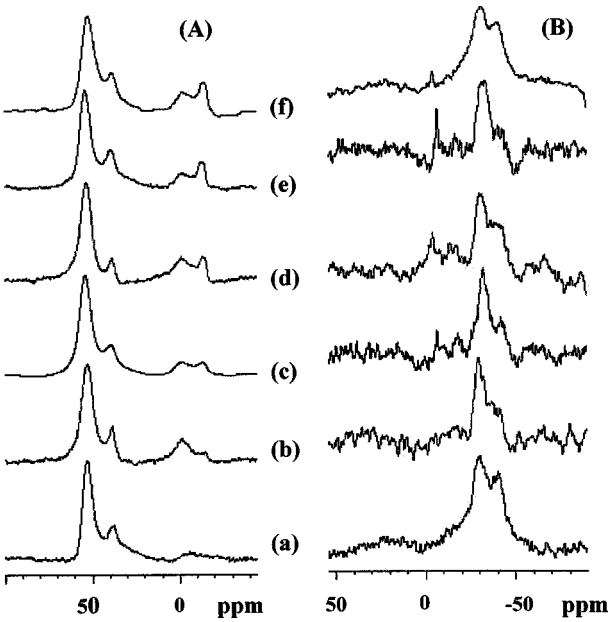

Figure 7. ^{27}Al (A) and ^{31}P (B) MAS NMR spectra of Mo/HZRP-1 catalysts calcined at 773 K: (a) HZRP-1, (b) 2Mo/HZRP-1, (c) 6Mo/HZRP-1, (d) 10Mo/HZRP-1, (e) 15Mo/HZRP-1 and (f) 20Mo/HZRP-1.

Table 2
The chemical shifts of ^{27}Al and ^{31}P MAS NMR spectra and assignment.

Chemical shift (ppm)	Assignment	Ref.
^{27} Al MAS NMR spectra		
53	Framework tetrahedral Al species coordinated with silicon	[10–14]
40	Framework tetrahedral Al atom related to the aluminophosphate phase	[10–14]
−1	Octahedral non-framework Al species	[10–14]
−15	Octahedral Al species in an aluminum phosphate phase or in an aluminum molybdate phase	[10–14]
^{31}P MAS NMR spectra		
−32	P atom related to the aluminophosphate phase	[11,12]
−40	P atom related to silicon pyrophosphate phase	[14]

3.3. *^{27}Al and ^{31}P MAS NMR spectra of Mo/HZRP-1 before and after reaction*

^{27}Al and ^{31}P MAS NMR spectra of the Mo/HZRP-1 catalysts with different Mo loadings, together with the HZRP-1 calcined at 773 K are shown in figure 7 (A) and (B). Referring to previous ^{27}Al and ^{31}P MAS NMR studies relating with P-modified catalysts published in the literature [10–14], the ^{27}Al and ^{31}P MAS NMR spectra recorded on the Mo/HZRP-1 catalysts can be reasonably assigned as listed in table 2. That at 53 ppm is typical for framework tetrahedral Al associating with silicon, and the other at 40 ppm is assigned to framework tetrahedral Al coordinating with phosphorus. The assignment of the peak at 40 ppm is confirmed by ^{31} P MAS NMR spectra of the Mo/HZRP-1 catalyst and is consistent with previous studies on phosphorus-modified catalysts [10–14]. The peak at −1 ppm is attributed to non-framework octahedral Al and still another peak at −15 ppm is assigned to aluminum molybdate phase. The intensities of the bands at 53, 40 and −1 ppm show slight changes, but the intensity of the band at −15 ppm increases with the increase of Mo loading. This implies that there is an extraction of framework Al atoms of the HZRP-1 by the Mo species, but it is not very strong. Even in the case of a Mo loading as high as 20%, the intensity of the band at −15 ppm is quite limited. With the increase of Mo loading, the ^{31}P MAS NMR spectra show that the band of −32 ppm changed slightly. This is in accordance with the change of the band at 40 ppm in figure 7(A). However, the variation of the silicon pyrophosphate phase is complicated, as we can see from the figure.

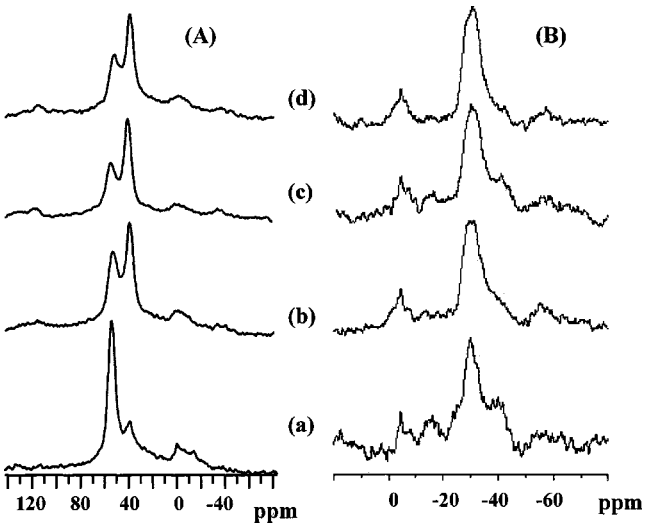

Figure 8. ^{27}Al (A) and ^{31}P (B) MAS NMR spectra of 6Mo/HZRP-1 after running for different on stream time under methane stream: (a) 0, (b) 60, (c) 180 and (d) 360 min.

^{27}Al MAS NMR spectra of the 6Mo/HZRP-1 catalysts after running the reaction for different time are presented in figure 8(A). For the 6Mo/HZRP-1 catalyst, the intensity of the band at 53 ppm decreased, while the band at 40 ppm intensified obviously after running the reaction for 1 h. With further increase of the reaction time, the intensity of the band at 53 ppm decreased continually while the band at 40 ppm intensified. This is due to the replacement of silicon by phosphorus such that the framework tetrahedral Al species associating with Si are transformed into the Al species relating to P under the reaction conditions. Moreover, this transformation is strengthened with the increase of reaction time. ^{31}P MAS NMR spectra of the 6Mo/HZRP-1 catalyst after reaction are presented in figure 8(B). The intensity of the band at −32 ppm increased, while the band at −40 ppm almost disappeared after running the reaction for 1 h. This is in consistent with the variation of the 40 ppm peak with the reaction time in ^{27}Al MAS NMR spectra.

4. Discussion

4.1. Comparison of the catalytic performances of the Mo/HZRP-1 and the Mo/HZSM-5 catalysts

The reaction results of Mo/HZRP-1 and Mo/HZSM-5 after running 30 min under the same reaction conditions are shown in figure 9. The results show that as a modification of the HZSM-5, the zeolite HZRP-1 is also a good support for the preparation of Mo/HZRP-1, and is active for methane dehydro-aromatization, especially at high Mo loading, as shown in figure 9. The rates r_{BTX} and r_{NA} on Mo/HZRP-1 increase rapidly in the Mo range of 0–6%, and then increase slightly in the range of 6–20%. It is interesting to note r_{BTX} over 6Mo/HZRP-1 catalyst is less than that over 20Mo/HZRP-1 catalyst, while r_{NA} over the 6Mo/HZRP-1 is higher than that over the 20Mo/HZRP-1 after running the reaction for 30 min. In contrast with the low Mo loading catalysts, the high Mo loading catalysts will lead to a decrease in the channel space available for the evolution, formation and diffusion of bulky molecules such as naphthalene, resulting in higher light aromatics formation. Indeed, the micropore volume decreases about 40% with the introduction of 20% Mo as evidenced with BET measurement. NH_3-TPD reveals the area of peak H of the 20Mo/HZRP-1 is much lower than that of the 6Mo/HZRP-1 as shown in table 1. Therefore, it is reasonable to assume that Mo species close to the Brønsted acid sites are responsible for the formation of light aromatics, in addition to the Brønsted acid sites unmodified by Mo species. r_C on 20Mo/HZRP-1 is higher than that on 6Mo/HZRP-1 at the early stage of the reaction. It implies that not only the Brønsted acid sites, but also the Mo species, either on the external or in the internal surface, are responsible for the formation of carbonaceous deposits.

Both r_{BTX} and r_{NA} decrease more quickly on 20Mo/HZRP-1 than on 6Mo/HZRP-1 after running the reaction for 6 h. Again, it shows that the change of effective diameter of the channel exerts a serious effect on the formation, evolution and diffusion of product molecules. The formation of carbonaceous deposits on Mo/HZRP-1 in the reaction further decreases the effective diameter of the channel.

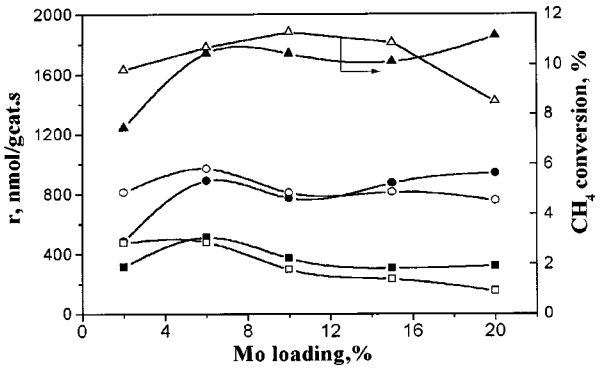

Figure 9. A comparison of catalytic performances over Mo/HZRP-1 (solid symbols) and Mo/HZSM-5 (empty symbols) catalysts: (△, ▲) conversion of methane, (○, ●) r_{BTX} and (□, ■) r_{NA}.

It is obvious that Mo/HZSM-5 shows better catalytic performance at low Mo loading than Mo/HZRP-1, while Mo/HZRP-1 exhibits better catalytic performance at high Mo loading. The HZRP-1 zeolite can accommodate more Mo species and keep higher reactivity. This is possibly due to its better stability of the HZRP-1 zeolite framework at high Mo loading.

4.2. The role of the framework tetrahedral Al species

The relationship between acid sites and the formation rates of light aromatics and naphthalene is an interesting subject. In their study on the titled reaction, Lunsford et al. suggested that the catalytic activity is directly proportional to the amount of Brønsted acid sites [15]. These sites are responsible for the oligomerization and dehydrocyclization of the primary product ethylene. Correlating the reaction results (figure 5) with the ^{27}Al MAS NMR spectra (figure 8(A)), it is obvious that with the decrease of the intensity of the peak at 53 ppm on the 6Mo/HZRP-1, r_{CH_4}, r_{BTX} and r_{NA} decrease. Unfortunately, because of the complicated nature of the ^{27}Al MAS NMR spectra, it is impossible to correlate the reaction rates with the intensity of the band at 53 ppm, but a parallel relationship between the rates and the intensity of the band is obvious. There is another kind of tetrahedrally coordinated Al in HZRP-1 at the band of 40 ppm which coordinate with phosphorus as the ^{27}Al MAS NMR spectra revealed. For the 6Mo/HZRP-1 catalyst, after running the reaction for 1 h, the intensity of the band at 53 ppm decreased, while the band at 40 ppm intensified obviously. With further increase of the reaction time, the intensity of the band at 53 ppm decreased continually while the band at 40 ppm intensified. Therefore, our results are in good agreement with Lunsford et al. [15] that the tetrahedrally coordinated Al atoms in the form of Al–O–Si species in the zeolites, in their proton forms (i.e., the Brønsted acid sites), are the sites closely related to the reactivity of the methane dehydro-aromatization. The other kind of framework Al atom coordinated to P atom is not active for the reaction.

5. Conclusion

(1) As a modification of HZSM-5, HZRP-1 is also a good support for the preparation of Mo-based zeolite catalysts, and is active for methane dehydro-aromatization. Mo/HZRP-1 catalysts are more active at high Mo loading, as compared with Mo/HZSM-5 catalysts.

(2) In addition to the Brønsted acid sites unmodified by Mo species, the Mo species in the channel close to the Brønsted acid sites are also responsible for the formation of light aromatics. On the other hand, not only the Brønsted acid sites, but also the Mo species, either on the external or in the internal surface, are responsible for the formation of carbonaceous deposits.

(3) There are two kinds of tetrahedral Al in the framework of HZRP-1. It is suggested the framework tetrahedral

coordinated Al atoms in the form of Al–O–Si species in the zeolite, in their proton forms (the Brønsted acid sites), be an important component of the active sites responsible for methane dehydro-aromatization.

Acknowledgement

Financial support from the Ministry of Science and Technology of China under the contract of G1999022400 is gratefully acknowledged.

References

[1] Y. Xu and L. Lin, Appl. Catal. A 188 (1999) 53.
[2] A. Szöke and F. Solymosi, Appl. Catal. A 142 (1996) 361.
[3] F. Solymosi, J. Cserényi, A. Szöke, T. Bansagi and A. Oszké, J. Catal. 165 (1997) 150.
[4] D. Wang, J.H. Lunsford and M.P. Rosynek, Topics Catal. 3 (1996) 289.
[5] D. Wang, J.H. Lunsford and M.P. Rosynek, J. Catal. 169 (1997) 347.
[6] R.W. Borry III, E.C. Lu, Y. Ho Kim and E. Iglesia, Stud. Surf. Sci. Catal. 119 (1998) 403.
[7] D. Ma, Y. Shu, X. Bao and Y. Xu, J. Catal. 189 (2000) 314.
[8] X. Shu, W. Fu, M. He, M. Zhou, Z. Shi and S. Zhang, US Patent 5 232 675 (1993).
[9] Y. Shu, Y. Xu, S. Wong, L. Wang and X. Guo, J. Catal. 170 (1997) 11.
[10] J. Sanz, J.M. Campelo and J.M. Marinas, J. Catal. 130 (1991) 642.
[11] E.C. Decanio, J.C. Edwards, T.R. Scalzo, D.A. Storm and J.W. Bruno, J. Catal. 132 (1991) 498.
[12] I. Hannus, I. Kiricsi, P. Fejes, A. Fonseca, J.B. Nagy, W.O. Parker, Jr. and Z. Szendi, Zeolites 16 (1996) 142.
[13] T.R. Krawietz, P. Lin, K.E. Lotterhos, P.D. Torres, D. Barich, A. Clearfield and J.F. Haw, J. Am. Chem. Soc. 120 (1998) 8502.
[14] B.A. Morrow, S.J. Lang and I.D. Gay, Langmuir 10 (1994) 757.
[15] B.M. Weckhuysen, D. Wang, M.P. Rosynek and J.H. Lunsford, J. Catal. 175 (1998) 338